

Reflective attenuator for high-energy laser measurements

John H. Lehman,* David Livigni, Xiaoyu Li, Christopher L. Cromer, and Marla L. Dowell

National Institute of Standards and Technology, Laser Radiometry, 325 Broadway, Boulder, Colorado 80305, USA

*Corresponding author: lehman@boulder.nist.gov

Received 26 March 2008; accepted 5 May 2008;
posted 20 May 2008 (Doc. ID 94239); published 17 June 2008

A high-energy laser attenuator in the range of 250 mJ (20 ns pulse width, 10 Hz repetition rate, 1064 nm wavelength) is described. The optical elements that constitute the attenuator are mirrors with relatively low reflectance, oriented at a 45° angle of incidence. By combining three pairs of mirrors, the incoming radiation is collinear and has the same polarization orientation as the exit. We present damage testing and polarization-dependent reflectance measurements for 1064 nm laser light at 45° angle of incidence for molybdenum, silicon carbide, and copper mirrors. A six element, 74 times (18 dB) attenuator is presented as an example. © 2008 Optical Society of America

OCIS codes: 140.0140, 140.3330, 230.0230.

1. Introduction

A laser attenuator having a well-known and stable attenuation can extend the usefulness of an optical power meter for laser radiometry. High-power laser radiometry ($\sim\text{kW}/\text{cm}^2$) is typically undertaken with a thermal detector having a sensor such as a thermopile and an optical absorber such as a ceramic disk. The usefulness of a calibrated thermal detector may be limited because the sensor is inherently nonlinear and has small dynamic range or because its absorber has a low damage threshold [1]. A calibrated attenuator must have minimal backscatter and a high damage threshold, and not influence polarization and amplitude stability of the laser light. We describe the design, calibration, and uncertainty assessment of a novel attenuator for measurement of laser power and energy.

There are several strategies for building optical attenuators, including the use of absorbing glass (transmissive) or partial reflectors (reflective) [2]. Passive attenuators, such as a neutral-density filter, or active attenuators, such as a tunable liquid crystal, have been studied [3]. The challenge of building attenua-

tors for high-power laser measurements (kW/cm^2 and greater) is to minimize damage and instability from heating. In practice, the usefulness of an absorbing glass or other neutral-density attenuator is limited because of nonlinearity and permanent damage from heating [4]. However, an absorbing glass is convenient compared to other alternatives because such an optical element will not significantly alter the state of the attenuated beam other than to reduce the optical power. This is preferred over other passive methods, such as a beam splitter or polarizer, which may alter the beam path or polarization of the laser energy.

Coated mirrors have a disadvantage for our application because we have found that the reflectance changes when heated, which is likely when used with a *Q*-switched neodymium-doped yttrium aluminum garnet (YAG) laser beam, for example [2]. For this reason, avoiding optical surfaces having a dielectric coating, although not a strict requirement, was among the design goals. Uncoated isotropic metal mirrors are known to have good thermal stability with respect to reflectance [5]. However, our choices for a range of reflectance are limited by the number of stable metals that have a high laser damage threshold and that may be mechanically machined and polished.

We have investigated the use of reflective attenuators with multiple reflective surfaces, each with

relatively high absorption. The design goal was to distribute the total attenuation and absorption among optical elements (partial reflectors), thus achieving the convenience of a transmission attenuator and the thermal stability of a reflective attenuator. Figure 1 is a schematic of such an attenuator. The strategy is an adaptation of a trap detector design described previously [6]. The advantages of the multiple reflection trap are no (or small) back reflection, high energy or power capability, long-term stability, small polarization sensitivity, and ease of alignment. For six surfaces, the total attenuation is

$$A = (\rho_1\rho_2\rho_3\rho_4\rho_5\rho_6)^{-1}, \quad (1)$$

where ρ_n is the reflectance of each surface. The small polarization sensitivity is attributable to the fact that an incoming beam encounters three *s*-polarization and three *p*-polarization reflections. Therefore, the ensemble of six surfaces will not alter the incoming polarization only if each surface is oriented at a 45° angle of incidence. We describe the reflectance measurements and damage assessment of the individual mirror elements followed by the attenuation factor and the components that contribute to the uncertainty of the attenuation factor, such as scattering.

2. Mirror Reflectance

The reflectances of three mirror materials (molybdenum, silicon carbide, and copper) were measured at an angle of incidence of 45°. Each mirror was illuminated with linearly polarized laser light having a nominal center vacuum wavelength of 1064.193±0.012 nm, contained in an approximately Gaussian beam with nominal $1/e^2$ intensity diameter of 2 mm and power of 1 mW [7]. The reflectance was determined from the ratio of the output of two identical germanium detectors (identified as detector 1 and detector 2). For each reflectance measurement, the mirror was translated into and out of the beam path directed at detector 1. Detector 2 measured the reflected beam. The ratio of the outputs of detector 1 and detector 2 defines the reflectance. This measurement was repeated several times, then the detectors were exchanged and the measurements repeated again to define another ratio. The geometric mean

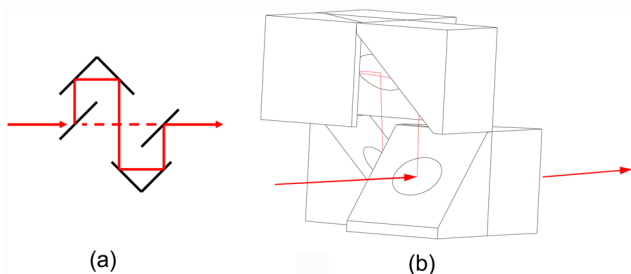


Fig. 1. (Color online) Representation of a reflective attenuator with six mirror surfaces. (a) Inset shows schematically that the light (indicated by arrow) is reflected at a 45° angle of incidence. The input beam is collinear with the output. (b) The relationship of the reflecting surfaces with respect to the transmitted beam.

of the two ratios (R1, R2) was then calculated to account for differences in the two detectors. In every instance, the expanded uncertainty of the reflectance measurement was less than 0.52%. The results of the three mirrors are summarized in Table 1.

3. Damage Threshold

Each mirror sample was mounted in a test fixture such that the angle of incidence of the laser was 45°. The laser energy at 1064 nm, (20 ns, 10 Hz pulses) was continually monitored for stability by sampling a portion of the beam reflected by a beam splitter. The reflected beam was directed at a reference detector at normal incidence to monitor the reflected laser energy. The circular beam size was determined to have a nominal diameter of ~7 mm, as determined by varying the aperture size such that 99% of the laser energy was contained within the area defined by the 7 mm aperture. The energy of the laser was incrementally raised until the laser energy on the reference detector was smaller than the average, which indicates the change in reflectance because of laser damage. This threshold was consistent with the appearance of a blemish on the mirror surface. The uncertainty of the damage measurement has not been thoroughly evaluated. It can be stated that the reference thermopile, calibrated with the designated National Institute of Standards and Technology (NIST) calibration service, is capable of measurements having an uncertainty of ~1.2%. The uncertainty of the damage threshold, however, depends strongly on the laser beam uniformity. Repeated damage experiments on witness samples that were considered to be nominally the same ranged in magnitude by 15%. The data, presented in Table 2, are provided as a design guideline rather than a definitive material property. The value in Table 2 of “greater than 250 mJ” is the upper limit of the laser used for the measurement. In other words, we were unable to damage the silicon carbide and copper mirrors at the operating limit of our laser with a 7 mm beam diameter.

4. Attenuator Study

The attenuator was assembled from three pairs of mirrors, copper, silicon carbide, and molybdenum. The attenuator was measured by use of the system shown in Fig. 2. The calibration was obtained by measuring the laser power incident on a reference detector, with and without the attenuator in the

Table 1. Reflectance Measurement Results

Material	Polarization	Reflectance 45°
Molybdenum	<i>s</i>	0.7865
	<i>p</i>	0.6240
Silicon carbide	<i>s</i>	0.3088
	<i>p</i>	0.0992
Copper	<i>s</i>	0.9792
	<i>p</i>	0.9795

Table 2. Summary of the Approximate Damage Thresholds of the Mirror Components

Material	Damage Threshold
Molybdenum	200 mJ
Silicon carbide	> 250 mJ
Copper	> 250 mJ

beam path. If the attenuator is placed in the beam path of a 1064 nm laser, the output power (on average) is equal to the input power divided by the average attenuation of 74.58. The calibration was accomplished with a linearly polarized solid-state laser having a nominal center vacuum wavelength of 1064.193 ± 0.012 nm, contained in an approximately Gaussian beam with nominal $1/e^2$ intensity diameter of 2 mm and power of 1 mW. The transmitted power was measured by use of a NIST internal transfer standard.

The expanded uncertainty of the overall attenuation is summarized in Table 3, where type A uncertainties are attained by statistical analysis and S_r is the standard deviation of a representative data set of N samples. The type B uncertainty and the magnitude of σ_r are estimated to fall within a rectangular distribution centered on the value of the overall attenuation. Alignment related to spatial uniformity is based on assessment of the spatial variability of the attenuation over the clear aperture. In this case, the aperture size is 17 mm, which is based on the circular projected area of a 25 mm diameter mirror at a 45° angle of incidence. The uncertainty in angle of incidence is based on alignment of the attenuator aperture with respect to the incoming beam to account for the nonideal alignment and the incoming beam is not oriented centered and perpendicular to the aperture plane. Polarization uncertainty is based on the fact that the s and p reflectances diverge greatly at a 45° angle of incidence. Therefore, slight misalignment of one of the individual mirror elements (of each pair) with respect to the incoming beam will result in one polarization being reflected more or less than it would by its complementary partner. The contribution of electrical instrumentation is merely that which accounts for the precision of the instrumentation for measuring the electrical signal from the de-

tor. The measurement repeatability is a value representing the extent to which the overall attenuation factor is the same from one independent measurement to the next. The temperature dependence is not accounted for in Table 3, but it is an important consideration. The temperature of the optical surfaces on the input side of the attenuator (silicon carbide in this case) may increase substantially from rapid heating by a laser pulse. Measurements of silicon carbide reflectance with heating in addition to that induced by the laser indicate no change in the average attenuation (or reflectance) up to an average temperature of 50°C . At temperatures $>50^\circ\text{C}$, the change in the overall attenuation before the onset of irreversible damage has not been evaluated. The additional uncertainty is described in greater detail in the text that follows.

The scattering uncertainty was determined by measurements of optical power in an annular area outside the $1/e^2$ beam diameter, with and without the attenuator present. This is presented as a type B estimate to quantify the amount of optical power that is cumulatively scattered by the mirror surfaces in the attenuator. In this test, a detector with circular limiting apertures having diameters from 3 to 10 mm was placed in the beam path. The attenuator was in the far field of the Gaussian beam waist with a full width beam divergence angle of ~ 1.2 mrad. In the absence of the attenuator the detector was translated along the optical path by a distance of 17.2 cm to accommodate the attenuator path length. The amount of power received by the detector through the given aperture was measured and normalized to the optical power measured for a 1 cm aperture. This approach is justified on the basis of the observation that the measurable optical power at 1 cm diameter is asymptotically approaching zero. The uncertainty of the scatter is calculated from a piecewise integration of the aperture area defined by radius R and the optical power, P , with and without the attenuator. That is, the scattered power may be expressed as

$$P_{\text{scatter}} = P_a - P_{\text{na}}, \quad (2)$$

Table 3. Measurement Uncertainties and Relative Expanded Uncertainty of the Attenuation Factor

Source	Type B σ_s	Type A S_r
Parameters Related to Attenuation		
Detector linearity (%)	0.0015	
Scatter (%)	0.015	
Spatial uniformity (%) ($N = 441$)		0.443
Alignment related to spatial uniformity (%)	0.02	
Angle of incidence (%)	0.10	
Attenuation		
Polarization	0.21	
Electrical instrumentation	0.10	
Measurement repeatability ($N = 7$)		0.1089
Relative Expanded Uncertainty ($k = 2$)		1.03%

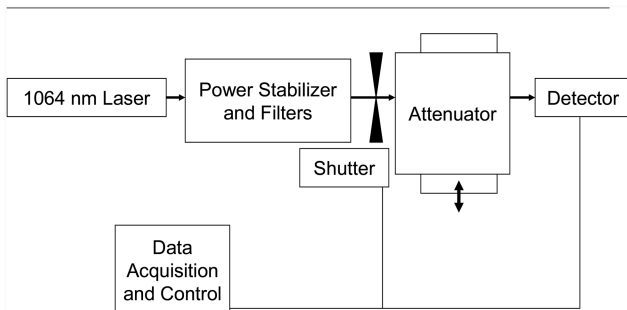


Fig. 2. Schematic relationship of the attenuator measurement equipment. The attenuator is moved in and out of the beam path to determine the attenuation factor.

where P_a is the power with the attenuator present and P_{na} is the power without the attenuator present in the annular area greater than the $1/e^2$ beam diameter and less than 1 cm. In terms of the measured power as a function of aperture radius r ,

$$P_{\text{scatter}} = \frac{2 \int_{R_i}^{R_o} r(P_a - P_{na}) dr}{R_o^2 - R_i^2} \quad (3)$$

is the power in the annular area defined by inner radius R_i (at $1/e^2$ beam radius) and outer radius R_o (1 cm aperture radius).

The spatial uniformity was acquired by sampling the attenuator aperture in a two-dimensional array. A laser beam with approximately Gaussian intensity profile was scanned across the face of the attenuator at spatial increments of 0.5 mm. The attenuator's transmittance was measured relative to that in the attenuator's center and expressed as a percentage of the transmittance in the center. The uncertainty contribution attributable to variations in spatial uniformity is a percentage of the average attenuation stated in Table 3.

5. Discussion

We expect the attenuation to be 69.39 based on calculations using values in Table 1 and Eq. (3). We measured, however, the ensemble attenuation to be 74.58. Based on the uncertainty assessment described earlier, scattering alone does not account for the difference. The data provided in Table 1 are typical and not necessarily the reflectance of the mirrors incorporated into the attenuator. The reflectance of any one mirror may vary from sample to sample due to variations in surface quality and homogeneity of the bulk. Discussions with mirror manufacturers support the idea that the reflectance of mirror specimens will vary from sample to sample. In some cases, the manufacturer's specifications may claim reflectance values only at a 45° angle of incidence with uncertainties as high as $\pm 5\%$. We believe this is conservative for high-purity, uncoated metal mirrors. For the current discussion we present this information merely for the sake of argument and not as a general conclusion about mirror reflectance. The point is that the mirror reflectance will vary slightly from piece to piece and this variation will determine the overall attenuation factor of the ensemble. As an example, if the representative mirror reflectance used in calculation differs from the actual reflectance by 1%, the calculated attenuation factor will differ from the measured value by more than 6%.

Knowledge of the reflectance of the individual mirror components, based on either data in the literature or our own experiments, is useful for the sake of designing the attenuator and to narrow the many possible combinations of materials. We made the effort to measure sample properties and to use sample measurement results because the reflectances calculated from the refractive index values in the literature are either unavailable or unsuitable

for indeterminate alloys [8]. The reflectance we calculated using data from the literature for nominally identified materials did not match our experimental results well enough to make design decisions. This may be because what we call molybdenum may in fact be an alloy designed to minimize oxidation. In the end, however, agreement with values in the literature is not critical and whether the attenuation factor is 70 or 75 is not as important as the repeatability, long-term stability, and resistance to damage.

6. Conclusion

We have designed a laser attenuator based on the sequential partial reflection of a collimated beam at a 45° angle of incidence. The mirrors are arranged with respect to the incoming radiation such that the input and output beams are collinear and the incoming polarization is unaltered. By selecting pairs of uncoated silicon carbide, molybdenum, and copper mirrors we are able to achieve an overall attenuation factor of approximately 74 with a damage threshold exceeding 250 mJ per pulse. With an accurate value of the overall attenuation, the attenuator can be used to extend the dynamic range of a calibrated laser power meter with only a small additional uncertainty. In the future, by choosing other types of mirror pairs, we can increase or decrease the attenuation factor. For example, our calculations using Eq. (1) indicate that incorporating silicon carbide (two pairs) and copper (one pair), we can achieve an attenuation factor of approximately 1000. The attenuator has the advantage over traditional attenuator techniques because of thermal stability, polarization insensitivity, and minimal back reflection.

We thank the Air Force Primary Standards Laboratory and the Department of Defense Calibration Coordination Group for support of this project.

References

1. X. Li, T. Scott, S. Yang, C. Cromer, and M. Dowell, "Nonlinearity measurements of high-power laser detectors at NIST," *J. Res. Natl. Inst. Stand. Technol.* **109**, 429–434 (2004).
2. R. O. Rice and J. D. Macomber, "Attenuation of giant laser pulses by absorbing filters," *Appl. Opt.* **14**, 2203–2206 (1975).
3. K. Hirabayashi, M. Wada, and C. Amano, "Compact optical-fiber variable attenuator arrays with polymer-network liquid crystals," *Appl. Opt.* **40**, 3509–3517 (2001).
4. D. L. Franzen and L. B. Schmidt, "Absolute reference calorimeter for measuring high power laser pulses," *Appl. Opt.* **15**, 3115–3122 (1976).
5. W. R. Goggin and J. W. Moberly, "Thermal dimensional instabilities of beryllium mirrors," *Appl. Opt.* **9**, 2691–2696 (1970).
6. J. H. Lehman and C. L. Cromer, "Optical tunnel trap detector for radiometric measurements," *Metrologia* **37**, 477–480 (2000).
7. By convention, the statement $1/e^2$ is to say that, for an ideally Gaussian laser beam profile, approximately 86% of the laser energy is contained within an area defined by the given radius.
8. E. D. Palik, *Handbook of Optical Constants of Solids II* (Academic, 1991).